A Multicoded-PPM Scheme for High Data Rate UWB Communication Systems

Sung-Yoon Jung and Dong-Jo Park

Abstract: **A new modulation scheme called multicoded-pulse position modulation (MC-PPM) is proposed for an ultrawideband (UWB) impulse radio communication system. The multicoded signal is generated by using several orthogonal codes for transmitting data simultaneously. Then, each multi-level value of the multicoded signal is converted to pulse position which results in not only an improved data rate, but also a processing gain in reception, delivering the power-efficient benefit of PPM and guaranteeing the low pulse energy for UWB systems. We notice that the modulation of multi-level values of the multicoded signal to pulse position is more efficient in terms of achievable data rate than the modulation of transmitting data based on other PPM schemes within given bandwidth and pulse energy. Therefore, as a performance measure, we focus on the achievable data rate (link capacity) of the proposed scheme and analyze it theoretically. Through simulation, we compare the link capacity of the MC-PPM scheme and other PPM schemes, such as M-ary PPM and multiple PPM. With the fixed bandwidth and same pulse energy condition, the UWB system based on the proposed MC-PPM scheme shows good link capacity and an increased data rate as L increases, which is contrary to other PPM schemes.**

Index Terms: **Link capacity, multicoded signal, pulse position modulation (PPM), ultrawideband (UWB).**

I. INTRODUCTION

Ultrawideband (UWB) radio communication is promising for applications in high data rate and short-range wireless communications, such as wireless personal area networks (WPAN). UWB systems are defined as any radio system that has a fractional bandwidth $\geq$ 0.20 or a UWB bandwidth $\geq$ 500 MHz regardless of the fractional bandwidth [1]. In accordance with the preliminary approval of UWB technology from the FCC first report and order, UWB systems are allowed to operate in the frequency band between 3.1 and 10.6 GHz for indoor UWB communication systems [2]. Theoretically, a UWB system can deliver a high data rate due to a large signal bandwidth. However, power spectrum density limitations, such as federal communications commission (FCC) Part 15 rules [2], limit the system capability. In particular, UWB systems under FCC Part 15 rules provide reliable communications only over small to medium distances.

UWB radio communication systems are usually referred to as impulse radios that transmit impulse-based waveforms occupying narrow pulse durations on the order of nanoseconds. Based on these impulses, many kinds of modulation schemes are used to transmit signals. The position or amplitude of the pulses, such as pulse position modulation (PPM) or pulse amplitude modulation (PAM) including antipodal signaling, is used to carry information [1], [3]. In all cases, one information bit is usually spread over multiple pulses to achieve a processing gain in reception because the power of the transmitted pulses is low in UWB radio systems. Among the various modulation schemes, the most commonly used for UWB impulse radio communication is PPM, especially binary PPM (BPPM) [4]–[5]. It is well known that PPM can achieve power efficiencies at the expense of bandwidth requirements [6]. Therefore, PPM fits well to the concept of UWB radio communications that requires low power instead of delivering a ultra-wide bandwidth. However, to apply this to a system that supports high data rates, the conventional BPPM scheme is not sufficient.

To increase the data rate of this scheme, either the pulse design or the modulation format needs to be considered. In [7], pulse shape modulation (PSM), based on orthogonal modified Hermite pulses combined with BPPM, is used. The data rate is increased with an increased size of the Hermite pulse set where each pulse in the set exhibits different spectral characteristics. This may lead to a requirement for different antenna structures, as well as violation of the spectral mask requirements as defined in the FCC first report and order. Another approach is to use M-ary PPM [8]. This modulation format increases the data rate at the expense of bandwidth expansion. However, if the bandwidth is fixed, the data rate in this scheme decreases while, conversely, increasing M. To overcome this drawback, there are activities to increase the data rate of the PPM scheme, such as multiple PPM (MPPM) [9]–[10]. MPPM uses two or more pulses to convey information. This can be accomplished by placing more than one pulse in all possible pulse positions and generating a much larger number of usable channel symbols when M is large. Till now, we discussed orthogonal PPM schemes, which basically assume that the pulse overlapping is not allowed. However, if we loose the restriction of orthogonal modulation, M-ary PPM scheme combined with pulse overlapping such as N-orthogonal PPM scheme is also possible [11]. However, it requires the optimized pulse design in additive white Gaussian noise (AWGN) and multipath channel taking into consideration the particular characteristic of UWB channel, which is not easy in practical implementation even though it does not violate the spectral mask requirement.

We propose a UWB impulse radio communication system based on multicoded-PPM (MC-PPM). The multicoded signal is generated by using several orthogonal codes for transmitting

Manuscript received November 28, 2007; approved for publication by Xuemin Shen, Division II Editor, October 21, 2008.

S.-Y. Jung is with the School of Electronic Engineering, Communication Engineering and Computer Science, Yeungnam University, 214-1 Dae-dong, Gyeongsan-si, Gyeongsangbuk-do, Korea 712-749, email: syjung@ynu.ac.kr.

D.-J. Park is with the School of Electrical Engineering and Computer Science, Korea Advanced Institute of Science and Technology (KAIST), 373-1 Guseong-dong, Yuseong-gu, Daejeon, Korea 305-701, email: djpark@ee.kaist.ac.kr.

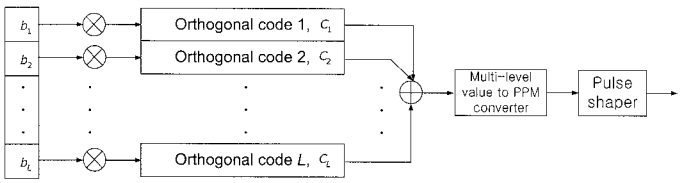

Fig. 1. The block diagram of the proposed MC-PPM scheme.

data simultaneously. Then, each multi-level value of the multicoded signal is converted to pulse position which results in not only an improved data rate, but also a processing gain in reception, delivering the power-efficient benefit of PPM and guaranteeing the low pulse energy for UWB systems. The proposed MC-PPM scheme does not change the spectrum, as in pulse shaping, nor does it expand the transmission bandwidth. Note that we do not consider pulse overlapping in order to focus on the modulation scheme itself, not the pulse design issue. This is because pulse overlapping scheme such as N-orthogonal PPM can also be combined with orthogonal PPM scheme if necessary. With the fixed bandwidth, no pulse overlapping and same pulse energy condition, the UWB system based on the proposed MC-PPM scheme shows good link capacity and an increased data rate as L increases, which is contrary to other PPM schemes such as M-ary PPM and multiple PPM.

The rest of paper is organized as follows. In Section II, we describe the proposed MC-PPM scheme. Performance is analyzed in Section III where, as a performance measure, we focus on the achievable data rate (link capacity) of the proposed MC-PPM scheme. Section IV presents simulation results in order to determine the validity of the proposed scheme. Through this, we show consistency of the analytical and simulated results and compare the link capacity of the proposed scheme with other PPM schemes, such as M-ary PPM and multiple PPM. Finally, conclusions are presented in Section V.

II. MC-PPM SCHEME

Fig. 1 shows a block diagram of the proposed MC-PPM scheme. As shown in the figure, each data block that contains L BPSK modulated data $\boldsymbol{b} = [b_1 \cdots b_L]^T$ is encoded by L binary orthogonal multicodes of length N to obtain a multicoded signal vector of length N, as follows:

$$\boldsymbol{d} = [d_1 \cdots d_N]^T = \boldsymbol{C}\boldsymbol{b} \tag{1}$$

where $\boldsymbol{C} = [\boldsymbol{c}_1 \cdots \boldsymbol{c}_L]$ is an $N \times L$ binary orthogonal code matrix and $\boldsymbol{c}_l = [c_{1,l} \cdots c_{N,l}]^T$, $c_{n,l} \in \{+1, -1\}$ denotes the lth orthogonal code. Then, each element of $\boldsymbol{d}$ has $L+1$ symmetric possible multi-level values, i.e., $d_n \in \{-L, -L+2, \cdots, L-2, L\}$.

A. Signaling Format

To transmit the signal, each element of a multicoded signal vector is converted to a pulse position vector as shown below:

$$\boldsymbol{m} = [m_1 \cdots m_N]^T \tag{2}$$

where $m_n = (d_n + L)/2$ denotes a delay for determining the pulse position. Note that we only need $L+1$ positions in order to transmit L data and this is the main feature which can increase the data rate in the proposed MC-PPM scheme. For multiple access, various schemes can be used, such as time-hopping multiple access (TH-MA) and direct sequence-multiple access (DS-MA) [12]. In this paper, we do not focus on the MA scheme. It is known that the gaussian approximation of multiple access interference is possible when the number of multiple access user is large [13]. Therefore, we omit the multiple access scheme and assume a single user case. After passing through a UWB pulse shaping filter, the transmitted UWB-IR signal based on multicoded PPM has the form

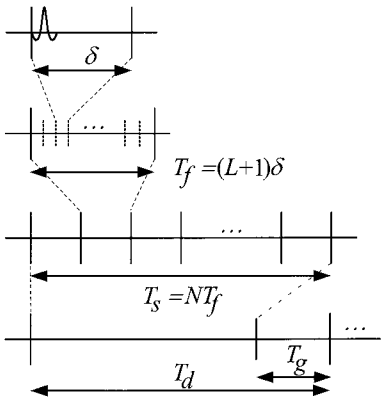

Fig. 2. The signaling structure of the proposed MC-PPM scheme.

$$x(t) = \sum_{i=-\infty}^{\infty} \sum_{n=0}^{N-1} \sqrt{E_w} w(t - iT_d - nT_f - m_n\delta) \tag{3}$$

where δ is the pulse spacing between two consecutive emission time slots, and $w(t)$ represents a normalized pulse of duration T_w and energy E_w. The transmitted signal that contains L data occupies a total of N frames of duration T_f and requires a time duration of $T_s = NT_f$ where $T_f = (L+1)\delta$. A guard time T_g remains at the end of transmission in order to consider the processing delay. Then, the total time duration required for transmitting a data block is $T_d = T_s + T_g$. The signaling structure of MC-PPM is shown in Fig. 2.

B. Receiver Design

The received signal $r(t)$ over a UWB multipath channel is given by

$$r(t) = x(t) \star h(t) + n(t) \tag{4}$$

where $n(t)$ is AWGN and $\star$ indicates the convolution operator. $h(t)$ is the channel impulse response modeled by [16] as below:

$$h(t) = \sum_{p=0}^{L_1} \sum_{q=0}^{L_2} \alpha_{p,q}\, \delta(t - T_p - \tau_{p,q}) \tag{5}$$

where $\{\alpha_{p,q}\}$ is the qth multipath gain coefficient of the pth cluster, $\{T_p\}$ is the delay of the pth cluster, and $\{\tau_{p,q}\}$ is the delay of the qth multipath component relative to the pth cluster arrival time (T_p). At the receiver end, we consider hard decision decoding, which is practical in real UWB communication systems due to implementation constraints related to the large system bandwidth. We also assume that the receiver is exactly synchronized

with the transmitter. Upon reception of $r(t)$, the receiver performs demodulation at the ith signal interval and produces the correlation metric $\boldsymbol{r}$ of length $(L+1)N_s$ as follows:

$$\boldsymbol{r} = [\boldsymbol{r}_0 \cdots \boldsymbol{r}_{N-1}]^T \tag{6}$$

$$\boldsymbol{r}_n = [r_{n,0} \cdots r_{n,L}]^T \tag{7}$$

where

$$r_{n,j} = \int_{iT_s+nT_f}^{iT_s+(n+1)T_f} r(t)\tilde{w}(t-j\delta)dt. \tag{8}$$

Here, $\tilde{w}(t)$ denotes the template pulse at the receiver, which can be implemented as either a coherent or noncoherent type. We assume that the pulse has the form $\tilde{w}(t) = w(t) \star h_R(t)$ and $h_R(t)$ can be

$$h_R(t) = \begin{cases} \hat{h}(t), & \text{for autocorrelation receiver} \\ \sum_{i=0}^{L_c} \beta_i \delta(t-\tau_i), & \text{for rake receiver} \end{cases} \tag{9}$$

where $\hat{h}(t)$ denotes the estimated channel and $\{\beta_i\}$, $\{\tau_i\}$, and L_c represent tap weights, tap delays, and the number of taps of the rake receiver, respectively [14].

Based on the maximum-likelihood (ML) decision rule, we detect the position of the transmitted pulses and regenerate the multicoded signal vector as shown below:

$$\hat{\boldsymbol{m}} = [\hat{m}_1 \cdots \hat{m}_N]^T, \tag{10}$$

$$\hat{\boldsymbol{d}} = [\hat{d}_1 \cdots \hat{d}_N]^T \tag{11}$$

where

$$\hat{m}_n = \arg \max_{j=0,\cdots,L} r_{n,j}, \tag{12}$$

$$\hat{d}_n = 2\hat{m}_n - L. \tag{13}$$

Finally, L data contained in $\hat{\boldsymbol{d}}$ are decoded by orthogonal codes used at the transmitter with the hard decision as follows:

$$\boldsymbol{z} = [z_1 \cdots z_L]^T = \boldsymbol{C}^T \hat{\boldsymbol{d}}, \tag{14}$$

$$\hat{\boldsymbol{b}} = [\hat{b}_1 \cdots \hat{b}_L]^T = \text{sign}\{\boldsymbol{z}\}. \tag{15}$$

III. PERFORMANCE ANALYSIS

The main purpose of the proposed approach is to enhance the data transmission rate of the system for high data rate UWB communication services. We notice that the key point, which can increase the data rate of the proposed scheme, is the conversion of multi-level values of the multicoded signal to pulse position. However, one of main concern is the effect of the proposed modulation scheme on the BER performance. Therefore, as a performance measure, we use the link capacity of the proposed scheme. Link capacity is simply a measure of how many bits per second can be transferred over a link [1] and it is represented as a function of the average bit error probability (BER) and the maximum data rate. Focusing on the link capacity, we analyze the achievable data rate of the proposed MC-PPM scheme.

A. Average BER Analysis

To evaluate the average BER performance, we derive the average error probability of the multicoded signal, P_e as the first step.

A.1 Error Probability of the Multicoded Signal

Noting that the position having a maximum value among $\{r_{n,j}\}_{j=0}^{L}$ is determined to be the transmitted symbol in the ML scheme, the correction probability given m_n is defined as

$$P_{c|m_n} = \int_{-\infty}^{\infty} P(E_{m_n}|m_n) p_{r_{n,m_n}} dr_{n,m_n} \tag{16}$$

where $P(E_{m_n}|m_n) = P(r_{n,m_n} > r_{n,j} \mid r_{n,m_n},\ j \neq m_n)$ is the probability that r_{n,m_n} is larger than each of the other L values $\{r_{n,j}\}_{j=0}^{L}$, $j \neq m_n$ when m_n is transmitted. Moreover, if the noise of each element in (4) is assumed to be independent, we can rewrite $P(E_{m_n}|m_n)$ as

$$P(E_{m_n}|m_n) = \prod_{j \neq m_n} P(r_{n,m_n} > r_{n,j} \mid r_{n,m_n}). \tag{17}$$

To complete the derivation of $P_{c|m_n}$, we need to know the probability density function (PDF) of each $r_{n,j}$ given m_n. By substituting (4) into (8), we can reformulate (8) as

$$\begin{aligned} r_{n,j} &= \mu_{n,j} + n_{n,j} \\ &= \begin{cases} \sqrt{E_w}\, R_{hh_R}(0) + n_{n,j}, & j = m_n \\ \sqrt{E_w}\, R_{hh_R}((j-m_n)\delta) + n_{n,j}, & \text{otherwise} \end{cases} \end{aligned} \tag{18}$$

where

$$R_{hh_R}(\tau) = \int_{-\infty}^{\infty} h(t) h_R(t-\tau) dt \tag{19}$$

and $n_{n,j}$ is filtered noise, which is also AWGN with a zero mean and a variance of σ_n^2. Then, the PDF of each $r_{n,j}$ can be derived from (18) as follows:

$$p_{r_{n,j}}(x) = \frac{1}{\sqrt{2\pi}\sigma_n} \exp\left[-\frac{(x-\mu_{n,j})^2}{2\sigma_n^2}\right]. \tag{20}$$

Using (20), $P(E_{m_n}|m_n)$ is given by

$$\begin{aligned} P(E_{m_n}|m_n) &= \prod_{j \neq m_n} \int_{-\infty}^{r_{n,m_n}} p_{r_{n,j}}\, dr_{n,j} \\ &= \prod_{j \neq m_n} \int_{-\infty}^{\frac{r_{n,m_n}-\mu_{n,j}}{\sigma_n}} \frac{1}{\sqrt{2\pi}} e^{-x^2/2}\, dx. \end{aligned} \tag{21}$$

Thus, the correction probability given m_n is

$$\begin{aligned} P_{c|m_n} = &\frac{1}{\sqrt{2\pi}} \int_{-\infty}^{\infty} \left[\prod_{j \neq m_n} \int_{-\infty}^{y} \frac{1}{\sqrt{2\pi}} e^{-x^2/2}\, dx\right] \\ &\cdot \exp\left[-\frac{1}{2}\left(y + \frac{\mu_{n,j} - \mu_{n,m_n}}{\sigma_n}\right)^2\right] dy \end{aligned} \tag{22}$$

and the probability of error given m_n will be

$$P_{e|m_n} = 1 - P_{c|m_n}. \tag{23}$$

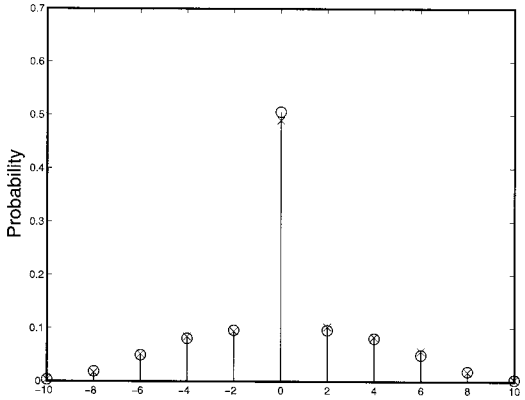

Fig. 3. The distribution of e_n when $L = 5, N = 8$, and $E_b/N_o = 0$ dB. (o: Analysis in (27), x: Simulation)

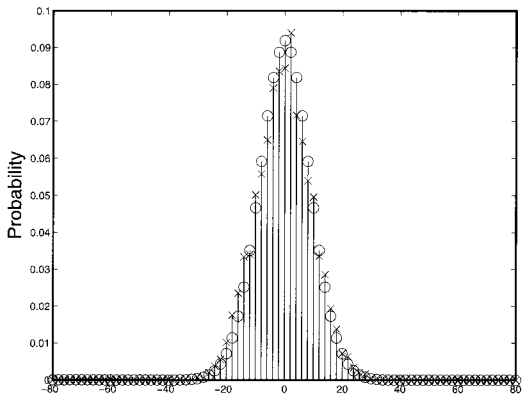

Fig. 4. The distribution of $\tilde{e}_l$ when $L = 5, N = 8$, and $E_b/N_o = 0$ dB. (o: Analysis in (30), x: Simulation)

Based on (23) and assuming the prior probability of m_n to be uniform, the average error probability of a multicoded signal, P_e is given by

$$P_e = \frac{1}{L+1} \sum_{m_n=0}^{L} P_{e|m_n}. \tag{24}$$

A.2 Average BER of the Multicoded-PPM

Using (24), we derive the average BER of the proposed multicoded-PPM scheme. To reach the objective, we first reformulate (11) as follows:

$$\hat{\boldsymbol{d}} = \boldsymbol{d} + \boldsymbol{e} \tag{25}$$

where $\boldsymbol{e} = [e_1 \cdots e_N]^T$ denotes the error vector due to detecting an incorrect pulse position in (10).

Then, the possible error values of each e_n according to d_n can be given as shown below:

$$\text{if } d_n = \begin{cases} L & \Rightarrow\ e_n \in E_{d_n} = \{0, -2, \cdots, -2L\} \\ L-2 & \Rightarrow\ e_n \in E_{d_n} = \{2, 0, \cdots, -2L+2\} \\ & \vdots \\ -L+2 & \Rightarrow\ e_n \in E_{d_n} = \{2L-2, \cdots, 0, -2\} \\ -L & \Rightarrow\ e_n \in E_{d_n} = \{2L, \cdots, 2, 0\}. \end{cases} \tag{26}$$

The probability distribution of each e_n can be formulated as follows:

$$\begin{aligned} p_{e_n}(r) &= \sum_{l \in D} P\{e_n = r | d_n = l\} P\{d_n = l\} \\ &= \begin{cases} 1 - P_e, & \text{for } r = 0 \\ \left[\sum_{i=0}^{L-|r|/2} {}_LC_i \left(\frac{1}{2}\right)^L\right] \frac{P_e}{L}, & \text{for } r \neq 0 \\ & \text{and } r \in \{-2L, -2L+2, \cdots, 2L\} \end{cases} \end{aligned} \tag{27}$$

where ${}_pC_q = \binom{p}{q} = \frac{p!}{q!(p-q)!}$ and $D = \{-L, -L+2, \cdots, -1+1, \cdots, L-2\}$. The detailed derivation of (27) is given in the Appendix. From (27), we can check that the mean of the distribution of e_n is zero and the variance $\sigma_{e_n}^2$ is given as

$$\begin{aligned} \sigma_{e_n}^2 &= \sum_{r=-2L}^{2L} r^2 p_{e_n} \\ &= \sum_{r=-2L}^{2L} r^2 \left[\left(\sum_{i=0}^{L-|r|/2} {}_LC_i \left(\frac{1}{2}\right)^{L-3} \right) \frac{P_e}{L} \right] \\ &\text{(letting } r = 2p,\ i = q \text{ with some modification)} \\ &= \left(\frac{1}{2}\right)^{L-3} \left[\sum_{p=0}^{L} p^2 \left(\sum_{q=0}^{L-p} {}_LC_q \right) \right] \frac{P_e}{L}. \end{aligned} \tag{28}$$

Fig. 3 shows the probability distribution of e_n when $L = 5$, $N = 8$, and $E_b/N_o = 0$ dB. From the figure, we can see that the derived distribution of e_n agrees with the simulation result. We used system parameters for the simulation that are described in Section IV.

Then, by using (1) and (25), we rewrite (14) as follows:

$$\begin{aligned} \boldsymbol{z} &= \boldsymbol{C}^T \hat{\boldsymbol{d}} = \boldsymbol{C}^T (\boldsymbol{d} + \boldsymbol{e}) \\ &= \boldsymbol{C}^T \boldsymbol{C} \boldsymbol{b} + \boldsymbol{C}^T \boldsymbol{e} = N \boldsymbol{b} + \tilde{\boldsymbol{e}} \end{aligned} \tag{29}$$

where $\boldsymbol{C}^T \boldsymbol{C} = N \boldsymbol{I}_L$ due to the orthogonal property of the code matrix $\boldsymbol{C}$ and $\boldsymbol{I}_L$ indicates the $L \times L$ identity matrix. $\tilde{\boldsymbol{e}} = [\tilde{e}_1 \cdots \tilde{e}_L]^T$ represents an error vector after the orthogonal decoding process. Here, each $\tilde{e}_l$ can be thought of as the sum of random variables $\{e_n\}_{n=1}^N$ because $\boldsymbol{C}$ is composed of binary orthogonal codes and the probability distribution of e_n has a symmetry property [(27) and Fig. 3]. Therefore, the distribution of each $\tilde{e}_l$ can be derived by convoluting the distribution of each e_n as shown below:

$$p_{\tilde{e}_l} = p_{e_1} \star p_{e_2} \star \cdots \star p_{e_N} \tag{30}$$

for all l. Assuming that each element of $\tilde{\boldsymbol{e}}$ is independent, the mean and the variance of $\tilde{\boldsymbol{e}}$ can be calculated as

$$\begin{aligned} \mathrm{E}\{\tilde{\boldsymbol{e}}\} &= \boldsymbol{0}_{L \times 1}, \\ \mathrm{var}\{\tilde{\boldsymbol{e}}\} &= N \sigma_{e_n}^2 \boldsymbol{I}_N. \end{aligned} \tag{31}$$

Fig. 4 shows the probability distribution of $\tilde{e}_l$ when $L = 5$, $N = 8$ and $E_b/N_o = 0$ dB. As shown in the figure, the derived distribution of $\tilde{e}_l$ agrees with the simulation results. From

(29), each element of $\boldsymbol{z}$ is written as

$$z_l = Nb_l + \tilde{e}_l, \qquad l = 1, \cdots, L. \tag{32}$$

If we let $P_b\{\text{error}|z_l\}$ denote the bit error probability of the lth bit, it is given by

$$\begin{aligned} P_b\{\text{error}|z_l\} &= P\{b_l = 1\}P\{\text{error}|z_l, b_l = 1\} \\ &\quad + P\{b_l = -1\}P\{\text{error}|z_l, b_l = -1\} \\ &= \frac{1}{2}\sum_{z_l=-\infty}^{0} p_{z_l|b_l=1} + \frac{1}{2}\sum_{z_l=0}^{\infty} p_{z_l|b_l=-1} \end{aligned} \tag{33}$$

where $p_{z_l|b_l=1}$ and $p_{z_l|b_l=-1}$ indicate the probability distributions of z_l when $b_l = 1$ and $b_l = -1$, respectively. These distributions act to shift the center of the probability distribution of $\tilde{e}_l$ to N when $b_l = 1$ and $-N$ when $b_l = -1$. Therefore, the average BER of the proposed multicoded-PPM can be derived as follows:

$$P_b = \frac{1}{L}\sum_{l=1}^{L} P_b\{\text{error}|z_l\}. \tag{34}$$

B. Link Capacity Analysis

To finalize the analysis of the link capacity, we derive the maximum data rate $R_{b,max}$ of the proposed multicoded-PPM scheme, represented as

$$R_{b,\max} = \frac{L}{T_d} = \frac{L}{N\,(L+1)\,\delta + T_g}\ (\text{bps}). \tag{35}$$

Then, from (34) and (35), the link capacity of the multicoded-PPM scheme is written as follows:

$$\begin{aligned} LC &= (1 - P_b)R_{b,\max} \\ &= (1 - P_b)\frac{L}{N\,(L+1)\,\delta + T_g}\ (\text{bps}). \end{aligned} \tag{36}$$

IV. SIMULATION RESULTS

We have described the proposed MC-PPM scheme and analyzed its performance. Now, we present analytical and simulated results and compare them with other PPM based schemes in order to determine the validity of the proposed scheme. For the simulations, we use the prolate pulse [17], which possesses a bandwidth of approximately 2 GHz, a center frequency of 4 GHz, and a time duration of approximately $T_w = 0.5$ ns.

The system parameters are also set to $T_m = 0.5$ ns and $T_g = 0$, and Walsh-Hadamard orthogonal codes are used for generating multicoded signals. The multipath channel is modelled as described in [16]. We assume that the receiver knows the channel state information. All simulation results are obtained by averaging 100 channel realizations, where 10,000 data blocks were generated for each channel realization.

Fig. 5 shows a comparison of the simulated and analytical results of the proposed scheme according to L when $N = 8$ on the AWGN channel. The analytical curves are matched with the simulation curves. Therefore, the analytical results provide a good estimation of performance when the system parameters have been selected. Even though the BER curves of the proposed MC-PPM scheme degrade as L increases, the performance gap becomes narrower in the high E_b/N_o region due to the processing gain of the proposed MC-PPM scheme caused by orthogonal multi-coding. In addition, we also notice that there is an increased link capacity as L increases under the fixed bandwidth and same pulse energy condition. This is the one of the main advantages of MC-PPM, which is not the case for other rate-enhanced PPM schemes.

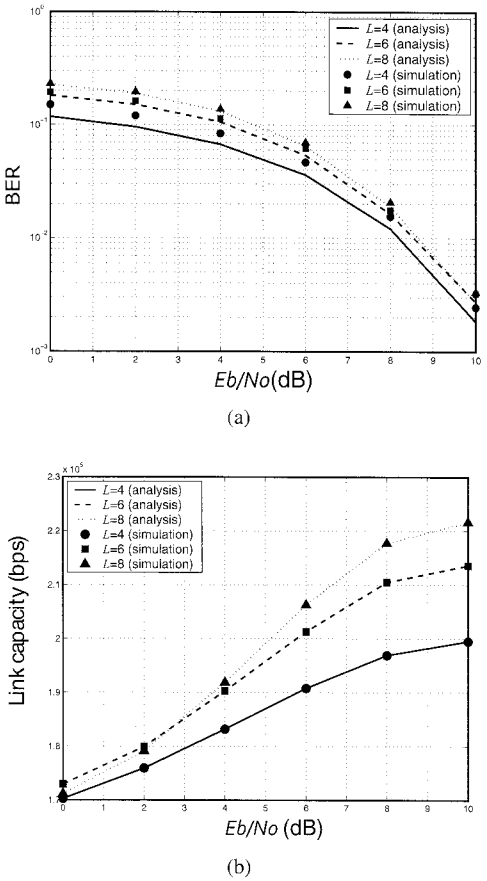

Fig. 5. The comparison between the simulated and analyzed performance of the proposed MC-PPM scheme: (a) BER and (b) link capacity.

Next, we compare the performance of the MC-PPM with other rate-enhanced PPM schemes. For other PPM schemes, we include M-ary PPM [8] and multiple PPM (MPPM), when the number of pulses was two [9]. They use a repetition code and hard-decision decoding for fair comparisons (the same pulse power, processing gain and detection rule) with the proposed MC-PPM scheme. In Fig. 6, we compare the performance of the proposed MC-PPM with that of M-ary PPM scheme when $L = 4, 8$, and $N = 8$ on the AWGN channel. As shown in Fig. 6(a), the BER performance of the proposed MC-PPM is worse than those of M-ary PPM in high E_b/N_o region. However, as shown in Fig. 6(b), the link capacity of MC-PPM is much higher than that of M-ary PPM scheme. It means that it is possible to compensate for the degraded BER performance of the proposed MC-PPM scheme in high E_b/N_o case by utilizing more powerful channel coding scheme with the benefit of higher data rate (similar comment is also mentioned in [11]).

In order to investigate a higher link capacity for the proposed

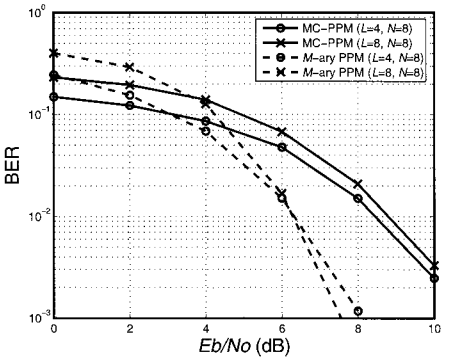

(a)

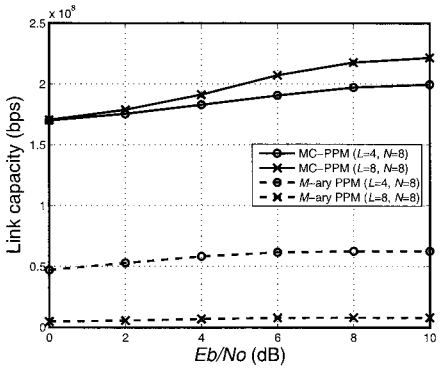

(b)

Fig. 6. The comparison of the performance between the proposed MC-PPM and M-ary PPM schemes: (a) BER and (b) link capacity.

Table 1. Simulation cases.

MC-PPM	L	1	2	4	8
	N	1	2	4	8
M-ary PPM	L	1	2	4	8
(no spreading)	N	1	1	1	1
M-ary PPM	L	1	2	4	8
(spreading)	N	1	2	4	8
Multiple PPM	L	1	2	4	8
(no spreading)	N	1	1	1	1
Multiple PPM	L	1	2	4	8
(spreading)	N	1	1	2	4

scheme, we compare link capacities of MC-PPM, M-ary PPM and multiple PPM schemes in the AWGN and multipath channels (CM1 and CM3). For CM1 and CM3, we use a rake receiver with maximum ratio combining (MRC) and the number of fingers set to 20 ($L_c = 20$). In addition, for M-ary PPM and multiple PPM, we consider 2 cases, 1) pulse spreading (pulse repetition) for distributing pulse energy in time (low pulse energy by the factor of processing gain per each pulse) and obtaining time diversity gain instead, 2) no pulse spreading. Note that we use walsh code, which can only increase its length as the power of 2, for orthogonal code in MC-PPM scheme. Therefore, we compare results as shown in Table 1. In Table 1, N is reduced to half in pulse spreading case of multiple PPM scheme (when the number of pulses is two) in order to satisfy same pulse

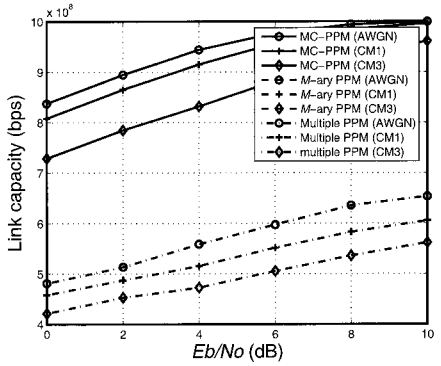

(a)

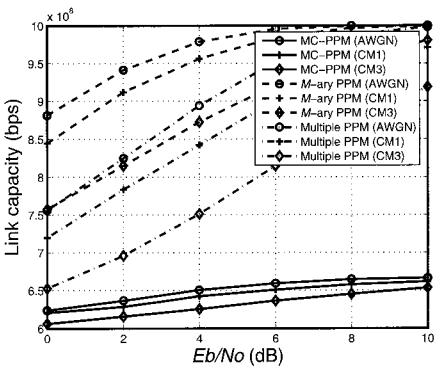

(b)

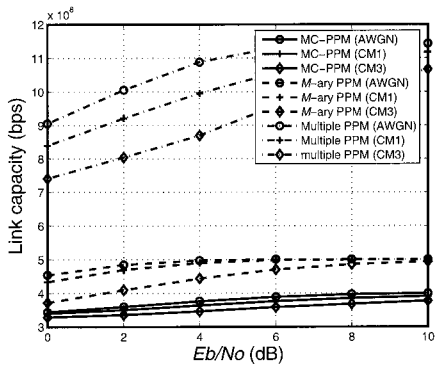

(c)

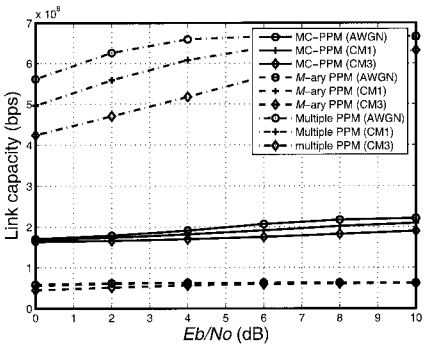

(d)

Fig. 7. The comparison of link capacity between the MC-PPM, M-ary PPM scheme and multiple PPM scheme according to L (no pulse spreading for M-ary PPM and multiple PPM: Larger pulse energy than that of MC-PPM): (a) $L = 1$, (b) $L = 2$, (c) $L = 4$, and (d) $L = 8$.

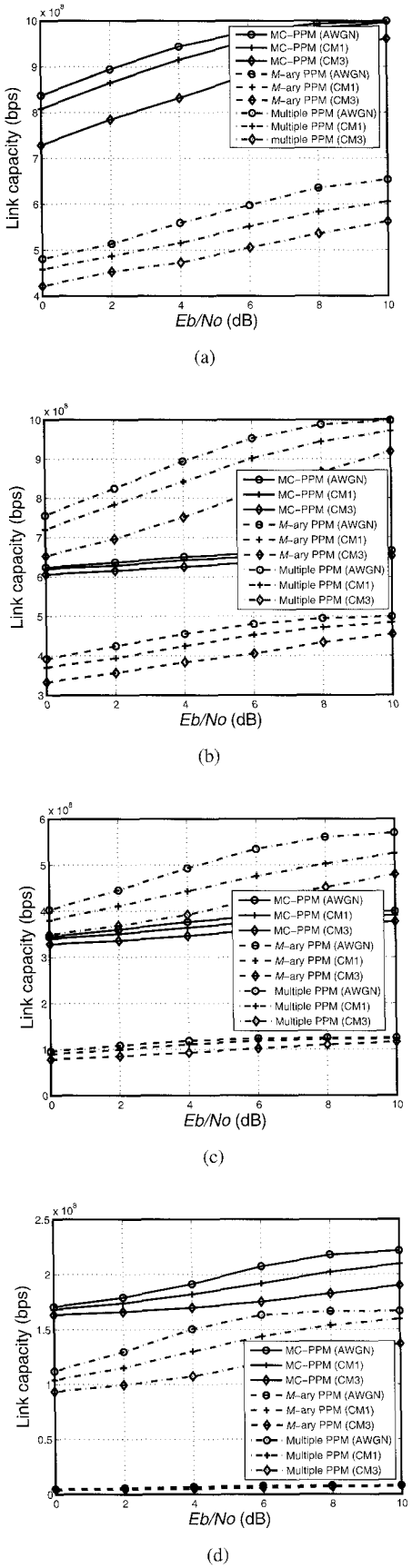

Fig. 8. The comparison of link capacity between the MC-PPM, M-ary PPM scheme and multiple PPM scheme according to L (pulse spreading for M-ary PPM and multiple PPM: Same pulse energy between all schemes): (a) $L = 1$, (b) $L = 2$, (c) $L = 4$, and (d) $L = 8$.

energy constraint with other schemes.

Fig. 7 shows the comparison of the link capacity when the pulse spreading is not used. From the figure, we can see that the link capacity of MC-PPM is going to be better than that of M-ary PPM when $L > 4$. In case of multiple PPM, it always shows higher link capacity than that of MC-PPM. However, note that the energy per pulse is N times ($N/2$ times) larger than that of MC-PPM in case of M-ary PPM (multiple PPM) due to no pulse spreading. In UWB communication systems, the pulse energy is low due to the spectral limitation of UWB. Therefore, it is desirable and widely used in the literature to adopt pulse spreading with multiple pulses to achieve a processing gain keeping low pulse energy in impulse radio based UWB schemes.

Otherwise, Fig. 8 shows the comparison of the link capacity when the pulse spreading is used. From the figure, it is clear that the link capacity of M-ary PPM is lower than that of MC-PPM regardless of L. In case of multiple PPM, it shows better performance than that of MC-PPM when $L < 4$ (except for $L = 1$), but getting worse as L becomes larger. Therefore, we can say that if we consider the low pulse energy in UWB system, it is desirable to spread energy by pulse repetition to achieve a processing gain in M-ary PPM and multiple PPM scheme. In that case, the link capacity of the proposed MC-PPM scheme shows good performance.

V. CONCLUSION

We have proposed a UWB impulse radio communication scheme based on multicoded-PPM. By converting multi-level values of the multicoded signal to pulse positions, we increased the data rate in PPM scheme while delivering the power-efficient advantage of PPM and guaranteeing the low pulse energy for UWB systems. Through analysis, we derived the link capacity of the MC-PPM scheme using average BER and maximum data rate in order to investigate the effect of data rate increase on the BER performance. Through simulations, we confirmed the consistency of the analysis with numerical results. In addition, we notice that with the fixed bandwidth and same pulse energy condition, the UWB system based on the proposed MC-PPM scheme shows good link capacity and an increased data rate as L increases, which is contrary to other PPM schemes.

APPENDICES

I. DETAILED EVALUATION OF (27)

We evaluate (27) in detail. The probability distribution of e_n is formulated as

$$p_{e_n}(r) = \sum_{l \in D} P\{e_n = r | d_n = l\} P\{d_n = l\} \qquad (37)$$

where $P\{d_n = l\}$ is the prior probability that the multicoded signal d_n is l, $P\{e_n = r|d_n = l\}$ indicates the conditional error probability of $e_n = r$ when $d_n = l$ and $D = \{-L, -L+2, \cdots, -1, +1, \cdots, L-2, L\}$. If we assume that orthogonal codes, which are used to generate the multicoded signal d_n in (1), are randomly generated with an equal probability and possible values $\{+1, -1\}$, it can be verified that $P\{d_n = l\}$ follows

the binomial distribution

$$P\{d_n = l\} = {}_L C_{(l+L)/2} \left(\frac{1}{2}\right)^L. \tag{38}$$

We also assume for analytical simplicity that the probability of each e_n to be r occurs with an equal probability. Then, the conditional error probability $P\{e_n = r|d_n = l\}$ can be written as

$$P\{e_n = r|d_n = l\} = \begin{cases} 1 - P_e, & \text{for } r = 0 \\ \frac{P_e}{L}, & \text{otherwise} \end{cases} \tag{39}$$

for all $d_n \in D$. By using (38) and (39), (37) is derived with some manipulation, as follows:

$$\begin{aligned} p_{e_n}(r) &= \sum_{l \in D} P\{e_n = r|d_n = l\} P\{d_n = l\} \\ &= \begin{cases} 1 - P_e, & \text{for } r = 0 \\ \left[\sum_{i=0}^{L-|r|/2} {}_L C_i \left(\frac{1}{2}\right)^L\right] \frac{P_e}{L}, & \text{and } r \neq 0 \\ & \text{for } r \in \{-2L, -2L+2, \cdots, 2L\}. \end{cases} \end{aligned} \tag{40}$$

REFERENCES

[1] K. Siwaik and D. Mckeown, *Ultra-Wideband Radio Technology*. John Wiley & Sons, Ltd., 2004.

[2] FCC ET Docket 98–153, "First report and order in the matter of revision of part 15 of the commission's rules regarding ultra-wideband transmission wystems," FCC 02–48, Apr. 2002.

[3] W. Zhuang, X. Shen, and Q. Bi, "Ultra-wideband wireless communications," *Wireless Commun. & Mobile Computing*, vol. 3, pp. 663–685, Sept. 2003.

[4] R. A. Scholtz, "Multiple access with time-hopping impulse modulation," in *Proc. IEEE Military Commun. Conf.*, Oct. 1993, pp. 447–450.

[5] M. Z. Win and R. A. Scholtz, "UWB TH-SSMA impulse radio for wireless multiple-access communication," *IEEE Trans. Commun.*, vol. 48, no. 4, pp. 679–691, Apr. 2000.

[6] J. G. Proakis, *Digital Communications*. 4th ed. McGraw-Hill, 2000.

[7] C. Mitchell and R. Kohno, "High data rate transmissions using orthogonal modified hermite pulses in UWB communications," in *Proc. ICT.*, Feb. 2003, pp. 1278–1283.

[8] F. Ramirez-Mirelez, "Performance of UWB SSMA using time hopping and M-ary PPM," *IEEE J. Sel. Areas Commun.*, vol. 19, no. 6, pp. 1186–1196, June 2001.

[9] M. K. Simon and V. A. Vilnrotter, "Performance analysis and tradoffs for dual-pulse PPM on optical communication channels with direct detection," *IEEE Trans. Commun.*, vol. 52, no. 11, pp. 1969–1979, Nov. 2004.

[10] F. Ono and H. Habuchi, "CDMA performance of the spread spectrum modified multipulse PPM system," in *Proc. WPMC.*, Oct. 2003.

[11] F. Ramirez-Mireles, "Performance of UWB N-orthogonal PPM in AWGN and multipath channels," *IEEE Trans. Veh. Technol.*, vol. 56, no. 3, pp. 1272–1285, May 2007.

[12] R. C. Qiu, H. Liu, and X. Shen, "Ultra-wideband for multiple access communications," *IEEE Commun. Mag.*, vol. 43, no. 2, pp. 80–87, Feb. 2005.

[13] N. V. Kokkalis, P. T. Mathiopoulos, G. K. Karagiannidis, and C. S. Koukourlis, "Performance analysis of M-ary PPM TH-UWB systems in the presence of MUI and timing jitter," *IEEE J. Sel. Areas Commun.*, vol. 24, no. 4, pp. 822–828, Apr. 2006

[14] J. D. Choi and W. E. Stark, "Performance of ultra-wideband communications with suboptimal receivers in multipath channels," *IEEE J. Sel. Areas Commun.*, vol. 20, no. 9, pp. 1754–1766, Dec. 2002.

[15] A. L. Garcia, *Probability and Random Processes for Electrical Engineering*. 2nd ed. Addison-Wesley, 1994.

[16] "Channel modeling sub-committee report final," IEEE P802. 15wg for WPANs, Feb. 2003.

[17] B. Parr, B. L. Cho, K. Wallace, and Z. Ding, "A novel ultra-wideband pulse design algorithm," *IEEE Commun. Lett.*, vol. 7, no. 5, pp. 219–221, May 2003.

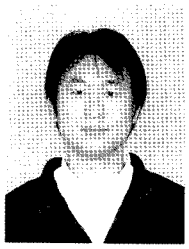

Sung-Yoon Jung received the B.S. degree from School of Electrical Engineering, Korea University, Seoul, Korea, in 2000 and the M.S. degree and Ph.D. in Electrical Engineering from the Korea Advanced Institute of Science and Technology (KAIST), Daejeon, Korea, in 2002 and 2006, respectively. He was a Senior Engineer in Telecommunication R&D Center, Samsung Electronics, Co., Ltd. in Suwon, Korea, from 2006 to 2009. He is currently a full-time Lecturer in the School of Electronic Engineering, Communication Engineering and Computer Science in Yeungnam University. His research interests include wireless personal area networks (WPAN) focusing on UWB communications, cooperative communications including MIMO, and relay scheme in OFDM(A) systems. He is a Member of IEEE, IEICE, and KICS.

Dong-Jo Park received the B.S. degree from the Department of Electrical Engineering, Seoul National University, Korea in 1976, and the M.S. and Ph.D. degrees in Electrical Engineering from the University of California, Los Angeles, in 1981 and 1984, respectively. He was a Senior Researcher of Electronics and Telecommunications Research Institute (ETRI), Daejeon, Korea, from 1984 to 1985. He is currently a Professor in the School of Electrical Engineering and Computer Science in the Korea Advanced Institute of Science and Technology (KAIST), Daejeon, Korea. His research interests include MIMO, OFDM, UWB, cooperative communication systems, and wireless multi-media signal processing. He is a Member of IEEE, IEICE, KIEE, KICS, and KISS.